

The effect of the material surface oxidation on laser light absorption

HRUŠKA Matěj, TESARĚ Jiří, VOSTŘÁK Marek, SMAZALOVÁ Eva

University of West Bohemia, Pilsen, Czech Republic, EU

maslej@ntc.zcu.cz, tesar@ntc.zcu.cz, mvostrak@ntc.zcu.cz, smazal@ntc.zcu.cz

Abstract. This study examines the influence of surface condition on its interaction with a laser beam. The relation was tested on milled C45 steel samples with a different width of created oxide layer. The milled surface with roughness 1.6 was modified by the creation of oxide layer. The oxide layers were created by solid state pulsed laser with scanning optics. The modified samples were processed by high power diode laser with a wide spread beam. The surface temperature was measured by the thermal camera during this process. The surface hardness and hardness depth profile were measured for all modified samples and the emissivity values were measured. The effect of pretreatment on hardness and microstructure will be discussed. The goal of this paper is to describe the relation between the parameters of created oxide layer and its effect on laser beam absorption.

1 Introduction

Laser hardening [1,2] is the modern technology of improving surface properties of the metallic materials. The material is rapidly heated to a high temperature by guiding the laser beam across the workpiece surface. Short interaction period of the laser beam and the processed surface cause, that the absorbed energy is concentrated only at the irradiated surface area, whereas the core remains cold. The rapid removal of heat from the surface layer to the colder unaffected bulk of a processed part allows the formation of a required microstructure. The used laser hardening technology is explained in [3].

The depth of hardened layer is dependent on absorbed energy. Dependence of hardened depth on various coatings was described in [4]. The relation between measured surface temperature and laser absorption was emphasized in this paper. An infrared camera was used in [5] for process characterization, control, and temperature field monitoring. ThermaCAM SC3000 was applied to temperature fields measurements during hardening of a cylinder in [6]. The view of the camera was at an angle of 30° with respect to the laser beam. The emissivity was set to the value of 0.88, corresponding to the applied surface coating, which was used to improve absorptivity. The same camera but at an angle of 53° was used in [7]. The emissivity of the sample was estimated during the heating with the propane torch in order to see how emissivity changes with temperature.

It is obvious that laser hardening is very closely connected with the surface condition because it can radically influence the absorption of a laser radiation. The absorption of the laser beam can be changed by modification of the optical properties of the irradiated sample surface. The modification can be achieved by pulsed laser processing. This method allows controlled growth of oxide layer. This phenomenon is described in detail in [8].

The incident, reflected, absorbed, and transmitted fluxes are connected together by energy conservation law. From this fact can be deduced that the sum of optical properties reflectivity (ρ), absorptivity (α), and transmissivity (τ) equals one [9]:

$$\rho + \alpha + \tau = 1 \quad (1)$$

For an opaque object without transmission ($\tau = 0$) the relation (1) simplifies

$$\rho + \alpha = 1 \quad (2)$$

Kirchhoff's law provides a relation between the absorption and emission processes and thus between emissivity and absorptivity

$$\varepsilon = \alpha \quad (3)$$

These relations are valid for similar spectral or total spectral condition. In this case, there are three sets of optical properties (three different wavelengths) for that Kirchhoff's law, is valid. The three wavelengths are the wavelength of engraving laser 1064 nm, the wavelength of hardening laser 808 nm, and the measuring range of infrared cameras 7.5 – 14 μm , eventually 1 μm . This means that, for example, the emissivity of the surface in the range of infrared camera ε_{IR} has no direct connection with absorptivity on the wavelength of hardening laser α_{HPDD} .

2 Experimental procedure

2.1 Surface modification process and absorptivity measurement

Tests were performed on a sample from milled steel C45 with roughness 1.6 and with a dimension of 100 x 100 x 25 mm. Oxide layers of square dimension 7 x 7 mm were created by marking laser SPI-G3-SP-20P with MOPA arrangement according to Figure 1. Parameters, to heating but not remelting the surface, were chosen. The scanning speed of the laser beam and the laser power were chosen common for all samples. The power was set to 17.25 W and the value of 800 mm/s was selected for scanning velocity. The depth of the oxide layer depends on energy E_v brought into the treated area. The quantum of the input energy was controlled by hatch density and allows operated growth of oxide layer. It means that it is controlled by the value of l_s distance between laser crossings. The manner of heating the treated surface layer by the laser is featured in Figure 2. 24 different oxide layers were made overall. Absorptivities of these 24 layers were measured in the ultraviolet (UV), visual (VIS), near-infrared (NIR) and mid-infrared (MIR) region. The method of measurement of spectral normal hemispherical reflectivity at room temperature was applied. FTIR spectrometer Nicolet 6700 and UV/Vis spectrophotometer Specord 210 BU were used for absorptivity measurement.

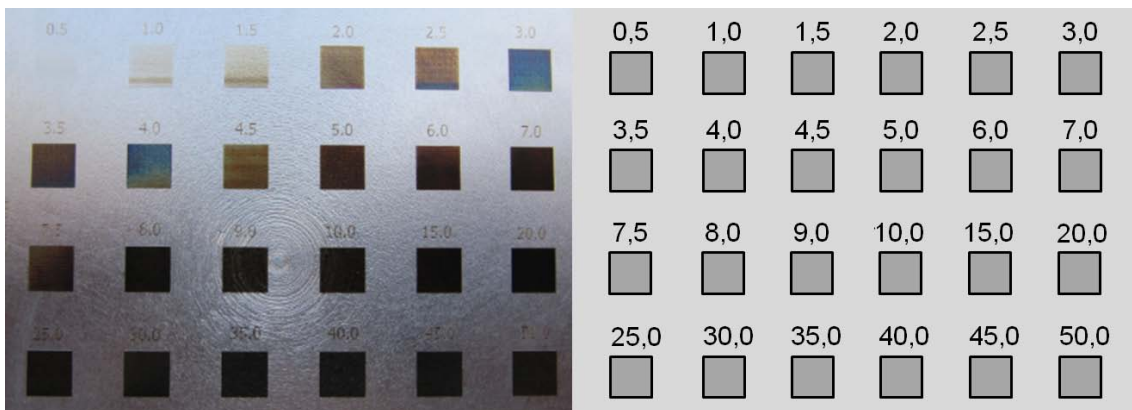


Figure 1 Sample after treating by marking laser (on the left), scheme of created oxide layers with used input energy values (on the right)

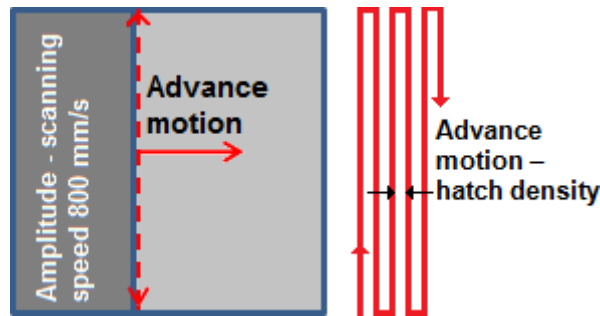


Figure 2 Technology of creating oxide layer by laser beam

2.2 Laser hardening process

The sample with treated squares undergoes consequently laser hardening with continuous HPDD (High Power Direct Diode) laser Coherent Highlight ISL – 4000L. The laser head is set on industrial manipulator Fanuc M710iC. The laser emits at wavelength 808 nm and its maximal power is 4.3 kW. The laser spot has a rectangular shape with dimension 12 x 6 mm, Gaussian energetic distribution in the 6 mm long side direction and uniform energetic distribution in the 12 mm long side direction. The laser beam with a power of 2 kW and traversing speed of 1.2 m/min was applied for processing of treated sample. The process was observed by three IR cameras (Figure 3).

The thermo-vision MSC640 was mounted on laser head to move with a laser beam. The camera measures emitted infrared radiation on the wavelengths around 1 μm (780 – 1080 nm) and had set temperature measurement range 673 – 1530°C. The thermo-visions Flir A615 and Variocam HD were set on tripods and these measures in the wavelength range 7.5 – 14 μm . The A615 camera has set temperature measurement range 100 – 650°C and the Variocam used 250 – 2000°C. The thermo-cameras measured with recording frequency 10 Hz. Measured values from the MSC640 were used for the evaluation, values from the other cameras have rather an informational character due to high emissivity dependence.

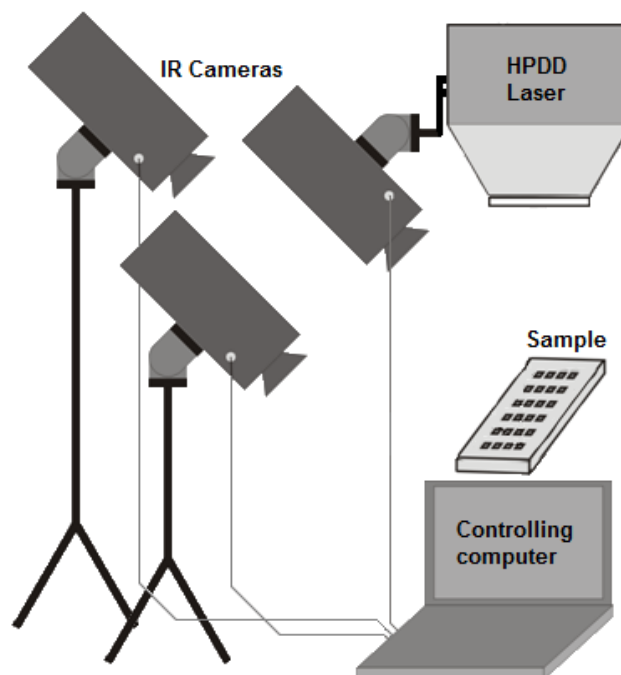


Figure 3 Experimental arrangement

3 Results and discussion

3.1 Temperature measurement and post-processing

The temperature was measured directly in laser spot during the hardening process. Temperature values were evaluated in LenaSense LumaSpec RT software the values were got by analyzing value at one point placed in the middle of the laser spot and the comparable value was obtained by averaging measured values from a whole laser spot area. The measurement by the MSC640 is significantly less dependent on the emissivity of the measured surface then using LWIR (Long Wave Infra Red) cameras because it measures infrared radiation on the wavelengths around 1 μm . The measurement accuracy of the thermo-vision is $\pm 0.5\%$ of measured value.

Table 1 Maximal temperatures – T_{max} and values obtained by averaging – T_{av} in relation to brought energy E_v (width of oxide layer), T_{max} , T_{av} (Figure 4) for non-treated surface flow along 1150–1200°C

E_v [J/mm ²]	0.5	1	1.5	2	2.5	3	3.5	4	4.5	5	6.1	7
T_{max} [°C]	1058	1097	1139	1206	1214	1256	1231	1238	1252	1267	1270	1307
T_{av} [°C]	1034	1076	1118	1191	1199	1253	1216	1229	1235	1260	1255	1305
E_v [J/mm ²]	7.5	8	9	10	15	20	25	30	35	40	45	50
T_{max} [°C]	1238	1303	1306	1327	1327	1389	1471	1442	1458	1451	1565	1643
T_{av} [°C]	1220	1274	1290	1292	1323	1376	1395	1405	1425	1428	1465	1583

The measured surface temperatures are shown in Table 1. One crossing of the sample by the laser beam is noted in Figure 4. Six variants of oxide layers with different width were overridden by the laser beam during this one crossing. The temperatures displayed in Figure 4 were measured for six different oxide layers created by laser heating with brought energy E_v from 25 to 50 J/mm². It is evident from Figure 4, that temperature measured on basic non-treated material flow maximally to 1200°C, the temperatures measured on treated areas flow along 1450 – 1650°C. Though the temperatures are above the melting point, the surface is not melted. The phenomenon can be caused by a measurement error of thermo-vision.

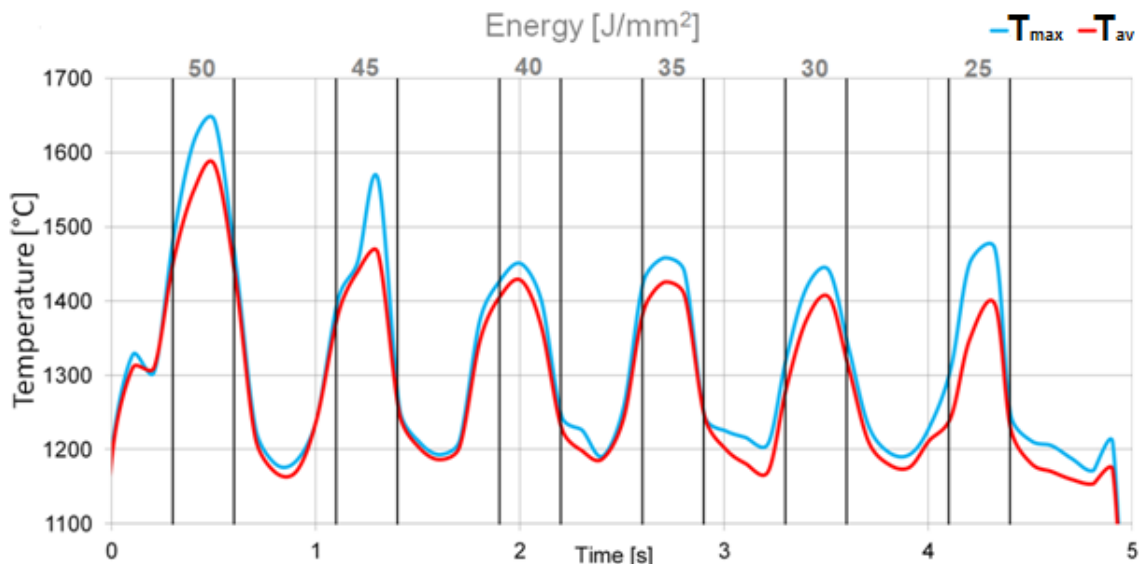


Figure 4 Compare – Temperature value analyzed from one point in the middle of the laser spot (blue line), Temperature value got by averaging measured values from a whole laser spot area (red line)

3.2. Microstructure and surface properties

Surface hardness and hardness depth profile were measured. The results in Tables 1, 2 implicate the relation between measured surface temperature and laser absorption that affects properties like surface

hardness and hardness depth. Higher surface temperature means higher laser absorption and higher laser absorption results in higher hardness depth. The surface temperature for laser hardening process has to exceed value 1050°C for C45 material to cause microstructure transformation and to assure the creation of required martensitic structure. Surface hardness decreases with the further gradual increase of surface temperature. It is caused by a decline in heat dissipation from the surface layer.

Table 2 Hardness measured 150 μm under the surface H_{150} and hardness depth profile H_D , for untreated surface $H_{150UN}=595 \text{ HV1}$, $H_{DUN}=400 \mu\text{m}$

E_v [J/mm^2]	0.5	1	1.5	2	2.5	3	3.5	4	4.5	5	6.1	7
H_{150} [HV1]	522	590	510	607	710	721	691	695	559	587	659	623
H_D [μm]	300	350	350	500	400	400	500	500	500	600	550	600
E_v [J/mm^2]	7.5	8	9	10	15	20	25	30	35	40	45	50
H_{150} [HV1]	710	678	649	620	706	637	710	713	675	702	774	683
H_D [μm]	550	600	650	600	500	500	550	500	650	650	600	700

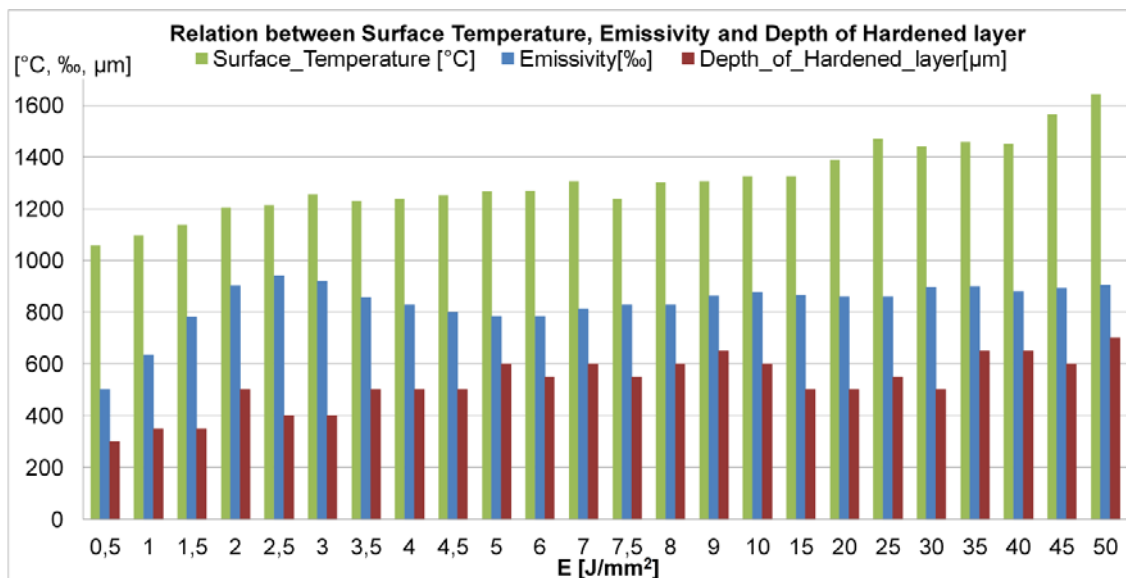


Figure 5 Compare of measured Hardness, Depth of hardened layer and Surface Temperature

The achieved depth of hardened layer depends on the surface emissivity. Notice that growing surface temperature results in increasing depth of the hardened layer of the irradiated surface. This upward trend can be seen in figure 5. The emissivity displayed in figure 5 was measured for 808 nm wavelength. The difference in the depth of hardened layer between the untreated surface and the treated area with the highest depth is around 300 μm . This result proves that the emissivity was seriously increased. The surface hardness of treated area was increased too.

This paper proves that thermal surface modification can seriously change absorptivity, resulting in the influence of the created hardened layer parameters.

4. Conclusion

The paper is focused on characterization of the relation between the surface absorptivity and its effect on the absorption of laser radiation during the hardening process. The absorptivity influences the surface temperature, measured during the process, and consequently parameters of formed hardened layer. The surface absorptivity can be changed by the creation of oxide layer. The width of the oxide layer depends on “brought energy”. “Brought energy” is input energy brought into the processed part. This input energy can be very precisely driven into the surface by using the IR laser beam and precious deflection system (scanning head). Higher input energy results in a higher depth of oxide layer [10] and thicker oxide layer causes higher absorption of laser radiation.

ACKNOWLEDGEMENTS

The result was developed within the CENTEM project, reg. no. CZ.1.05/2.1.00/03.0088, cofunded by the ERDF as part of the Ministry of Education, Youth and Sports OP RDI programme and, in the follow-up sustainability stage, supported through CENTEM PLUS (LO1402) by financial means from the Ministry of Education, Youth and Sports under the "National Sustainability Programme I." and project no. SGS-2016-005.

References

- [1] HRUŠKA, Matěj, VOSTŘÁK, Marek, SMAZALOVÁ, Eva, ŠVANTNER, Michal. Standard and scanning laser hardening procedure. *METAL International Conference on Metallurgy and Materials* [online]. 2013, s. 1009–1014. Dostupné z: http://apps.webofknowledge.com/full_record.do?product=UA&search_mode=Refine&qid=3&SID=U1nUP8aht9cZmirQKr2&page=1&doc=3
- [2] HRUŠKA, M., VOSTŘÁK, M., SMAZALOVÁ, E., ŠVANTNER, M. 3D scanning laser hardening. *METAL 2014 - 23rd International Conference on Metallurgy and Materials, Conference Proceedings*. 2014, s. 921–926.
- [3] KENNEDY, E., BYRNE, G., COLLINS, D. N. A review of the use of high power diode lasers in surface hardening. *Journal of Materials Processing Technology* [online]. 2004, roč. 155-156, č. 1-3, s. 1855–1860. ISSN 09240136. Dostupné z: doi:10.1016/j.jmatprotec.2004.04.276
- [4] Ways to Intensify Laser Hardening Technology. 1998, roč. 47, s. 133–136.
- [5] ATTIA, H., TAVAKOLI, S., VARGAS, R., THOMSON, V. Laser-assisted high-speed finish turning of superalloy Inconel 718 under dry conditions. *CIRP Annals - Manufacturing Technology* [online]. 2010, roč. 59, č. 1, s. 83–88. ISSN 00078506. Dostupné z: doi:10.1016/j.cirp.2010.03.093
- [6] PATWA, Rahul, SHIN, Yung C. Predictive modeling of laser hardening of AISI5150H steels. *International Journal of Machine Tools and Manufacture* [online]. 2007, roč. 47, č. 2, s. 307–320. ISSN 08906955. Dostupné z: doi:10.1016/j.ijmachtools.2006.03.016
- [7] SKVARENINA, Stephen, SHIN, Yung C. Predictive modeling and experimental results for laser hardening of AISI 1536 steel with complex geometric features by a high power diode laser. *Surface and Coatings Technology* [online]. 2006, roč. 201, č. 6, s. 2256–2269. ISSN 02578972. Dostupné z: doi:10.1016/j.surfcoat.2006.03.039
- [8] LAAKSO, P, RUOTSALAINEN, S, PANTSAR, H, PENTTILÄ, R. Relation of laser parameters in color marking of stainless steel [online]. 2009, s. 15. Dostupné z: http://www.vtt.fi/files/research/ism/manufacturingsystems/relation_of_laser_parameters_in_color_marking_of_stainless_steel.pdf
- [9] ROBERTO RINALDI, BORIS G. VAINER, PETR KUNC, IVANA KNIZKOVA, KLAUS GOTTSCHALK, GIOVANNI M. CARLOMAGNO, CHRISTOPHE ALLOUIS, ROCCO PAGLIARA, RALPH A. ROTOLANTE, ERMANNO GRINZATO, Carosena Meola. *Infrared Thermography (Recent Advances and Future Trends)*. B.m.: Carosena Meola, Department of Aerospace Engineering University of Naples Federico II, Italy, 2012. ISBN 9781608051434.
- [10] ADAMS, D. P. et al. Nanosecond pulsed laser irradiation of stainless steel 304L: Oxide growth and effects on underlying metal. *Surface and Coatings Technology* [online]. 2013, roč. 222, s. 1–8. ISSN 02578972. Dostupné z: doi:10.1016/j.surfcoat.2012.12.044